Microchim Acta (2016) 183:1055–1062
DOI 10.1007/s00604-015-1729-8

ORIGINAL PAPER

Enzyme-less and low-potential sensing of glucose using a glassy carbon electrode modified with palladium nanoparticles deposited on graphene-wrapped carbon nanotubes

Pranati Nayak[1,2] · **Santhosh P. Nair**[2] · **Sundara Ramaprabhu**[1]

Received: 3 September 2015 / Accepted: 10 December 2015 / Published online: 30 December 2015

Abstract The article describes an amperometric sensor for enzyme-less detection of glucose based on homogeneously anchored Pd nanoparticles (Pd-NPs) on graphene - wrapped carbon nanotubes (Pd-GWCNTs) as sensing matrix. The unique features of GWCNTs (such as the highly protruded outer graphene layer and an inner tubular morphology) result in enhanced electrochemical performance compared to the use of conventional multi walled carbon nanotubes (MWCNTs). Glucose electro-oxidation occurs at a rather low working potential (+50 mV vs Ag/AgCl), and glucose can be continuously sensed in 0.1 M NaOH solution in concentrations of up to 19.5 mM. The sensor possesses good reproducibility, a fast response time, stable amperometric response and a lower detection limit. Due to its low working potential, it is not interfered by dopamine, uric acid, ascorbic acid, sucrose, fructose and lactose. We presume that these beneficial properties are a result of the synergetic advantages of using catalytic Pd NPs and graphene wrapped CNTs, both of which facilitate low-potential electrooxidation of glucose.

Keywords Solar reduction · Glucose sensor · Nonenzymatic sensing · Electro-oxidation · Amperometry · Cyclic voltammetry · HRTEM · XPS · Raman spectroscopy

Electronic supplementary material The online version of this article (doi:10.1007/s00604-015-1729-8) contains supplementary material, which is available to authorized users.

✉ Sundara Ramaprabhu
ramp@iitm.ac.in

[1] Alternative Energy and Nanotechnology Laboratory (AENL), Nano Functional Materials Technology Centre (NFMTC), Chennai, India

[2] Low Temperature Physics Laboratory, Department of Physics, Indian Institute of Technology Madras, Chennai 600036, India

Introduction

The majority of sensors for glucose are based on the use of the enzyme glucose oxidase (GOx) along with optical or electrochemical transduction [1–3]. However, the use of enzymes complicates the sensor fabrication, limits the sensitivity stability and reproducibility of the sensor due to the intrinsic nature of enzyme, which is highly prone to be affected by temperature, pH, humidity and toxic chemicals [4, 5]. A promising strategy to these problems relies on the development of sensors based on direct glucose electrooxidation without using enzymes [6].

Though various nanostructure materials have been used in the design and fabrication of enzyme-less glucose sensors, noble metals are unprecedented catalysts due to their highly populated d-band, which readily participate in reactions leading to high catalytic activity [7]. Among common noble metal based catalysts, Pd-based nanomaterials have proven to be alternative electrochemical catalysts being considerably cheaper than platinum, the most frequently used catalyst in many applications [8]. Many approaches have been pursued to anchor the catalyst NPs on various nanoscopic-conducting substrates such as vulcan XC-72, carbon micro sphere (CMSs), hallow carbon spheres (HCSs), carbon fiber in order to prevent particle agglomeration enhance the catalytic activity and reduce the cost [9, 10]. However, the electrocatalytic performance relies not only on the catalyst and the support, but also the intimate contact between the NPs and the nanoscopic conducting substrate is imperative in facilitating the charge transport efficiency, which thereby promotes the electrocatalytic activity and intern favors low-potential glucose electrooxidation [11]. Carbon based nanostructures like CNTs and graphene have been emerging as an excellent support material as they share many novel properties such as high surface area, excellent electrical conductivity, huge electron mobility, chemical inertness and low cost [12]. Graphene

has gained incredible interest in electrochemical sensing because it is fairly stable, has large potential window and unprecedented surface properties for decorating other functional nanostructures [13]. On the other hand, the high aspect ratio and ballistic electron transport along their length of CNTs makes it as excellent nanoscale electrode materials for electrochemical sensing [14]. However, the rate of heterogeneous electron transfer (HET) in basal plane of sp^2 carbon network being 2–3 order slower than edge plane sites, the electrochemical activity at CNTs electrodes is mainly stemmed from the edge-plane-like nanotube tips [15, 16]. The highly oriented nanotube sidewall essentially remains inactive towards heterogeneous electron transfer reaction and is comparable to the basal plane of highly orientated pyrolytic graphite (HOPG). Similar to this, the highly roughen graphite surface exhibits better electrocatalysis compared to planar graphite surface. Very systematic investigations on this were reported in the landmark publications of Compton group [17, 18]. In this perspective, wrapping highly protruded graphene layers over CNTs (GWCNTs) opens up possibilities of enhanced electrochemical activity arising from the large number of edge-plane-like sites introduced by the wrinkles [19].

Here we report on the fabrication of a sensor platform based on Pd NPs anchored GWCNTs hybrid as sensing matrix for enzyme-less glucose electrooxidation. GWCNTs have been prepared by CVD technique using GO and catalyst as precursor. A facile, inexpensive, highly efficient and environmentally benign one-step solar reduction process has been employed for the decoration of Pd NPs over GWCNTs without using any harsh chemical reducing agents. The combined advantage of highly wrinkled sidewalls and anchored Pd NPs were proclaimed to be responsible for improved electrochemical activity. The detailed characteristic of the material ensures intimate contact between Pd NPs and GWCNTs with charge transfer interaction. The resulting hybrid was directly employed as sensing matrix for enzyme-less glucose detection, which exhibits an excellent sensing performance at a very low working potential.

Materials and methods

Materials

Flake graphite powder (99.99 % SP-1, average particle size 45 μm) was purchased from Bay carbon, Inc USA. Palladium(II) chloride hydrate ($PdCl_2$) and D-(+) glucose were purchased from Aldrich (www.sigmaaldrich.com). Sodium nitrate ($NaNO_3$), sodium hydroxide (NaOH), potassium permanganate ($KMnO_4$), concentrated sulphuric acid (H_2SO_4, 99 %), concentrated nitric acid (HNO_3, 98 %), were procured from Rankem chemicals, India (www.rankem.in) and used as received. Hydrogen peroxide (H_2O_2, 30 % wt/V) was purchased from Fisher scientific (www.thermofishersci.in). Dopamine, uric acid, L-Ascorbic acid, sucrose, lactose and fructose were procured from Alfa Aesar (www.alfa.com). All the chemicals used were of analytical reagent grade and used without further purification. All the electrochemical studies and synthesis has been done using ultrapure water (18.2 MΩ cm) from Millipore system (MilliQ).

Synthesis of materials

Graphite oxide (GO) was prepared by Hummer's method using natural flake graphite powder as the precursor (discussed in ESI) [20]. Graphene wrapping over MWCNTs has been done by catalytic chemical vapor deposition technique using 1:1 mixture of GO and rare earth based alloy ($MmNi_3$, Mm = Misch metal) catalyst [21]. The as synthesized GWCNTs were purified by air oxidising at 400 °C followed by refluxing in conc. HNO_3 in order to remove amorphous carbon and remaining metal catalyst particles. The Pd NPs decoration over GWCNTs was done by using focused sun light as the energy source to reduce Pd salt to Pd NPs following our earlier report [22]. Briefly a fine mechanical mixture of purified GWCNTs (100 mg) and palladium chloride (for 30 wt % loading) was prepared using a mortar and sprinkled in a glass petridisk. The mixture was irradiated by focused sun light using a convex lens of 90 mm diameter for 1–2 min. The rapid heating (about 100 °C/s) by lens creates sudden rise in temperature (150–450 °C), which decomposes the metal salt to metal NPs and simultaniously deposites on GWCNTs. An apparent release of gaseous byproducts were observed during synthesis, which indicate the decomposition of metal salt at high temperature. The synthesis procedure is described in the schematic shown in Fig. S1 (in Supporting Information).

Working electrode fabrication

The enzyme-less amperometric electrochemical sensor was fabricated by drop casting ultrasonically dispersed Pd-GWCNTs powder in Nafion solution (0.5 wt % solution in a mixture of lower aliphatic alcohols) on glassy carbon electrode (GCE, 2 mm diameter). The GCE was polished mirror like by 0.05 micron alumina slurry followed by rinsing thoroughly with DI water before fabrication. For preparing the modified electrode, about 20 μL of solution containing of Pd-GWCNTs (1 mg/0.1 mL in 0.5 % Nafion solution) was drop casted on the shining surface of the pre-treated GCE and allowed to dry at room temperature. The modified electrode can be named as Pd-GWCNTs@GCE for further studies. For comparison of the electrocatalytic activity of the hybrid nanocomposite, we prepared GWCNTs@GCE and MWCNTs@GCE taking the same weight percentage.

Material characterization techniques

The crystal structure of the synthesized products were studied by powder X-ray diffraction (XRD) analysis performed using PANalytica X'pert pro X-ray diffractometer in a range from 5 to 90° with a step size of 0.016° and Cu-K_α (1.54 Å) as X-ray source. The Raman spectra were recorded by WITec alpha 300 confocal Raman spectrometer equiped with Nd:YAG laser (532 nm) as excitation source and sample heating was avoided by exciting at low laser intensity. Thermogravimetric analysis was carried out in a SDTQ600 (TA instruments) in a zero air atmosphere from room temperature (30 °C) to 1000 °C with a heating rate of 20 °C/min. The morphology of the synthesized products were studied by Field emission scanning electron microscopy (FESEM, Quanta 3D) and High resolution transmission electron microscopy (HRTEM, Tecnai G^2 20 S-TWIN). X-ray photoelectron (XPS) spectra were recorded in order to investigate the chemical state of the products with SPECS X-ray photoelectron spectrometer using Mg K_α as X-ray source and PHOIBOS 100 MCD energy analyser at ultra high vacuum (10^{-10} mbar). The data were analysed using CASA XPS software. The electrochemical studies were performed by CH Instrument, electrochemical work station with a three electrode electrochemical cell comprising modified GCE as working electrode, Ag/AgCl (1 M KCl solution) as reference electrode and Pt wire as counter electrode. All the electrochemical measurements were carried out using 0.1 M NaOH solution as supporting electrolyte at ambient conditions.

Results and discussion

Characterization of Pd-GWCNTs composites

The electron microscopy technique has been employed to investigate the surface morphology of the synthesized nanocomposites. The FESEM images of purified GWCNTs at low and high magnifications are shown in Fig. S2 (a and b). It depicts disordered graphene layers over MWCNTs, which results a wrinkled morphology covering the entire surface with average diameter of ~100–120 nm and tens of micron length. Figure 1a exhibits the FESEM image of Pd nanoparticles anchred on GWCNTs surface at different magnifications. The TEM image (Fig. 1b) further affirm the successful uniform decoration of Pd NPs on GWCNTs. The FESEM and TEM images of Pd-GWCNTs at different resolution are shown in Fig. S2 (c, d, e and f) of ESI, which again confirms uniformity of anchored Pd NPs. Figure 1c shows the high resolution TEM image of a single Pd NP at 5 nm resolution, which depicts the inter plannar spacing for the lattice fringes of ~2.2 Å, which corresponds to <111> facet of Pd in cubic closed pack structure [23]. This confirms the good

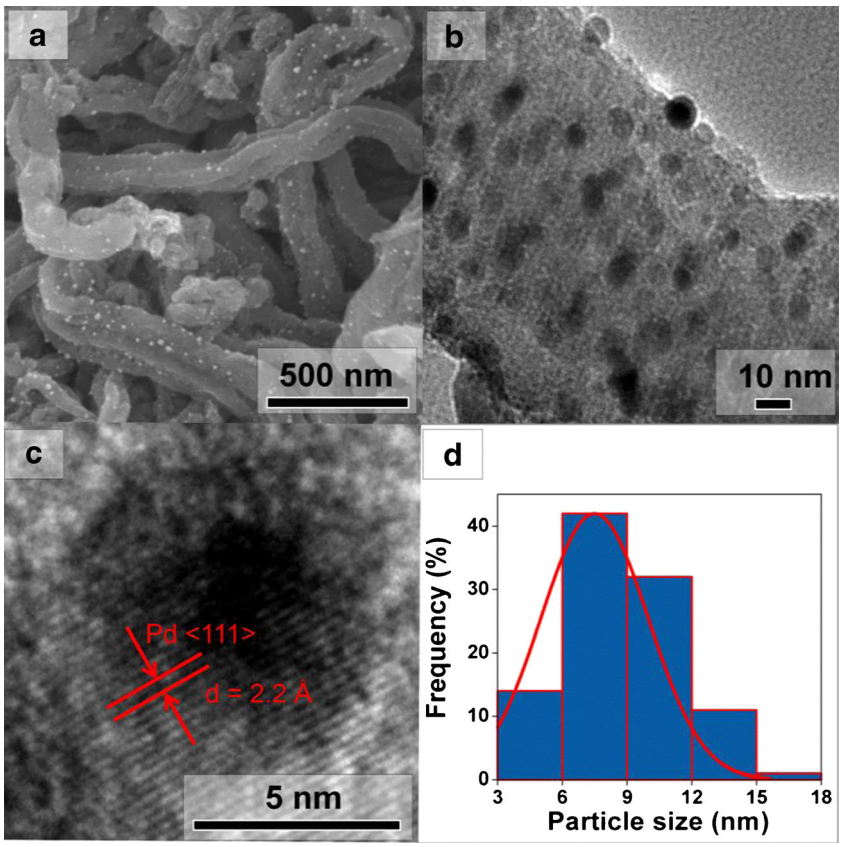

Fig. 1 (**a**) Field emission scanning electron micrograph (FESEM), (**b**) Transmission electron micrograph (TEM) and (**c**) high-resolution TEM micrograph of Pd-GWCNTs; (**d**) particle size histogram representing distribution of size of Pd nanoparticles

crystallinity of the Pd nanostructures over GWCNTs. The average particle size calculated from the particle size histogram (shown in Fig. 1d) is ~6–9 nm.

In order to affirm the successful formation and crystallinity of Pd NPs on GWCNTs, powder X-ray diffraction studies were carried out in the range from 5° to 90° with a step size of 0.016°. Figure 2a shows the XRD pattern of (a) Pd-GWCNTs compared to (b) pure GWCNTs. The characteristic peak corresponding to C (002) plane of hexagonal lattice for pure GWCNTs is observed at 26.42°. For Pd-GWCNTs, the diffraction peaks were identified to cubic lattice pattern of Pd (JCPDS 65–6174) along with C (002) peak. With the sharpness as well as the absence of any additional peaks corresponding to other oxidation states of Pd indicates complete conversion of Pd salt to Pd NPs and reflects the purity of the sample.

Raman spectroscopy is a powerful tool to investigate the interaction between surface decorated metal nanoparticles and the carboneous substrate by studying the charge-transfer mechanism. Figure 2b represents the Raman micrographs of (a) Pd-GWCNTs compared with (b) pure GWCNTs. For pure GWCNTs, peak at ~ 1580.7 cm^{-1} (G-band) corresponds to the E_{2g} vibration mode of graphitic carbon. The defect induced D band appears at ~ 1338 cm^{-1}, which are predominantly sensitive to the presence of disorder carbon atoms induced in graphitic structure and the surface modification by doping, etc. The intensity ratio of D and G band (I_D/I_G) is a measure to scale the defects on the modified structures [24]. Compared to pristine GWCNTs, the G band peak blue shifts for Pd-GWCNTs composites (shown as the high resolution spectrum in Fig. S3 of ESI). Again the intensity of 2D band decreases markedly up on Pd NPs decorations compared to pristine GWCNTs. These are the effect of columbic charge transfer between Pd NPs and GWCNTs and are the signature of intimate contact between Pd NPs and wrapped graphene surface, which intern enhances the electrocatalytic activity of the hybrid composite and favors low-potential glucose electrooxidation [25]. Again, being highly wrinkled surfaces, the D band intensity dominates over G band in GWCNTs with I_D/I_G ratio of ~ 1.39. The I_D/I_G value for Pd-GWCNTs is calculated to be 1.57, which further confirms attachment of Pd NPs on GWCNTs surface introducing more defects.

One of the advantages of the synthesis technique is the utilization of the whole precursor metal salt to convert to metal nanoparticles without giving any chemical by-products or residue, which is confirmed from TGA analysis (discussed in ESI). The loading of Pd NPs over GWCNTs is about ~30 wt % from the TGA spectra shown in Fig. S4 (in ESI). Further the quantitative information allied to the chemical state, type and composition of GWCNTs and Pd-GWCNTs hybrid composites are investigated by X-ray photoelectron spectroscopy (XPS) in binding energy ranging from 0 to 1000 eV (discussed in ESI, Fig. S5). The deconvoluted high resolution XPS spectrum for Pd 3d reveals a doublet at binding energies 335.5 eV (Pd $3d_{5/2}$) and 341.0 eV (Pd $3d_{3/2}$), which is shown in Fig. S5 (C). Other than these, peaks at 337.7, 339.5, 343.2 and 344.9 eV appears which are due to Pd-C_x bonding. The presence of Pd-C_x in the deconvoluted Pd 3d spectra indicates chemisorptions of carbon onto the palladium surface, which is highly prone to improve the electrocatalytic activity of Pd NPs [26, 27].

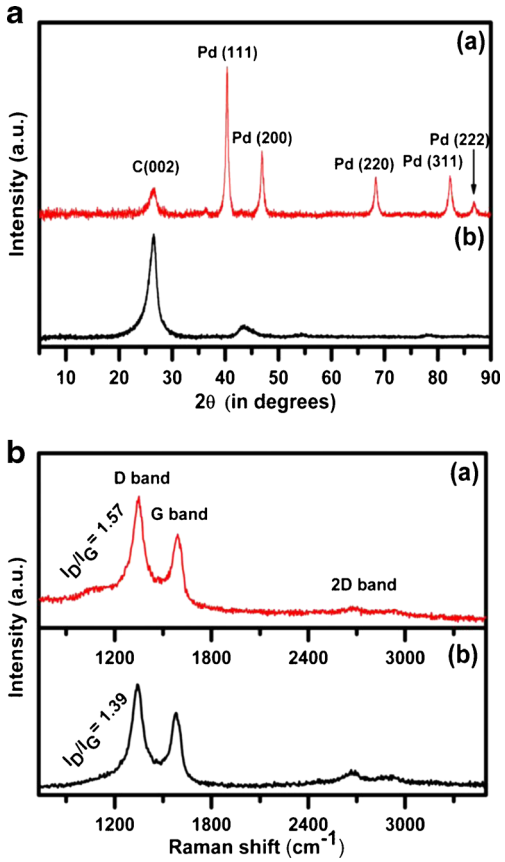

Fig. 2 (**a**) Powder XRD patterns and (**b**) Raman spectra of (**a**) Pd-GWCNTs compared with (**b**) GWCNTs

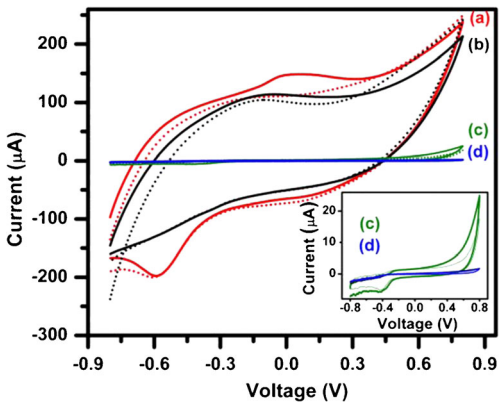

Fig. 3 CV response for (**a**) Pd-GWCNTs@GCE compared to (**b**) GWCNTs@GCE, (**c**) MWCNTs@GCE and (**d**) bare GCE in the presence (*solid line*) and in the absence (*dotted line*) of 5 mM glucose with 0.1 M NaOH as supporting electrolyte, scan rate: 50 $mV \cdot s^{-1}$. Insets: magnified plot for MWCNTs and bare GCE

Electrochemical performance study

The electrochemical performance of the modified electrodes towords glucose electroxidation was studied by cyclic voltammetry (CV) recorded in 0.1 M NaOH solution in the absence and presence of glucose. Figure 3 depicts the typical cyclic voltammograms for (a) Pd-GWCNTs@GCE, (b) GWCNTs@GCE, (c) MWCNTs@GCE and (d) bare GCE in the absence (dotted lines) and in the presence (solid lines) of 5 mM glucose at a scan rate of 50 mV/s. Inset shows the amplified CV plot for MWCNTs@GCE and bare GCE. Compared to bare GCE, MWCNTs@GCE gives more redox current due to high specific surface area and electrochemical activity. As observed, for GWCNTs@GCE the current genarated is enhanced compared to MWCNTs. This can be attriuted to the protruded graphene layers over MWCNTs surface, which avails more density of edge-plane like sites and enhnaces the electrochemical activity, thereby generates more current [28]. For Pd-GWCNTs@GCE, a wel defined oxidation current produces at a low oxidation potential of 0.05 V due to glucose electroxidation. This reveals the electrocatalytic activity of the Pd-GWCNTs@GCE towords glucose electroxidation. Again the CV was recorded on successive addition of 5 mM glucose, which reveals an increasing oxidation current due to glucose electroxidation (shown in Fig. S6 (a), ESI). Fig. S6 (b) depicts the comparision plot of current generated due to a fixed glucose concentration at different modified electrodes. Including this, it is followed that the current genarated due to glucose electroxidation covers a potential ranging from 0 to 0.2 V. In order to know the potential producing maximum current (I_p), we conducted a controlled experiment by investigating the amperometry behavior at different electrode potentials, as shown in Fig. 4a (a). For each addition of 1 mM glucose at different electrode potential, it is found that the maximum current genarates at a lower electrode potential of 0.05 V. Figure 4a (b) represents a maximum current vs. potential plot. Based on this i-t response of Pd-GWCNTs@GCE, the sensing behaviour was further evaluated by carring out calibration of the sensor.

Amperometric detection of glucose

In order to know the sensors activity towards different glucose concentration, the amperometry measurement was conducted for successive addition of glucose. Figure 4b depicts the amperometric (i-t) response for Pd-GWCNTs@GCE recorded at 0.05 V. As observed, each μM glucose injection results a proportionate increase in current and the plot follows step wise current enhancement. Inset shows the amplified i-t plot for addition of low glucose concentration. Figure 4c shows the calibration curve based on the amperometric response, which reveals excellent linear response up to 19.5 mM with regression equation as $y = 3.463\ x + 0.637$ and regression coefficient (R^2) of 0.998. Inset shows the linear behavior at low glucose

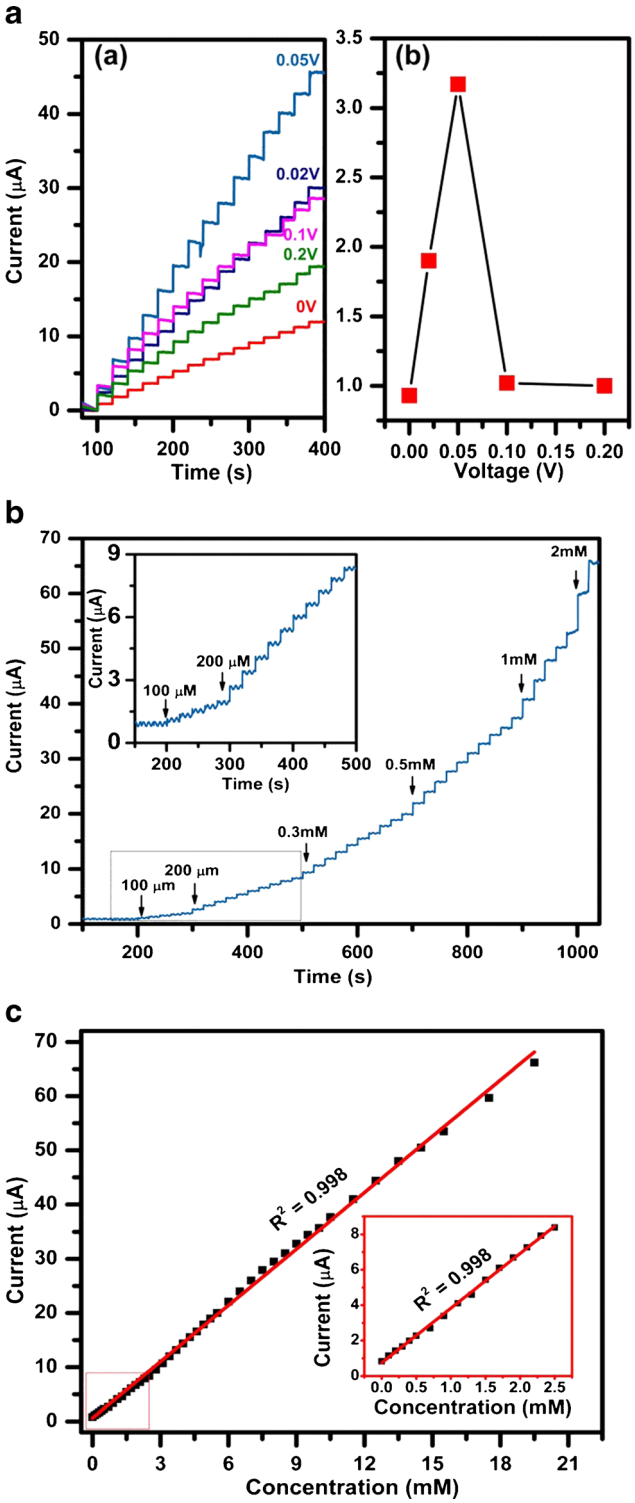

Fig. 4 **a** (*a*) Amperometric response of Pd-GWCNTs to successive addition of 1 mM glucose in 0.1 M NaOH at an applied potential of 0, 0.02, 0.05, 0.1 and 0.2 V (vs. Ag/AgCl reference electrode), (*b*) Effect of applied potential on the amperometric response of 1 mM glucose; **b** Amperometric response of Pd-GWCNTs@GCE to the successive addition of 100, 200 μM, 0.3 mM, 0.5 mM, 1 mM and 2 mM glucose in 0.1 M NaOH at an applied potential of 0.05 V (vs. Ag/AgCl reference electrode); **c** Linearly fitted calibration plot (steady state current versus glucose concentration), Insets: showing linearly fitted plots in lower concentration region

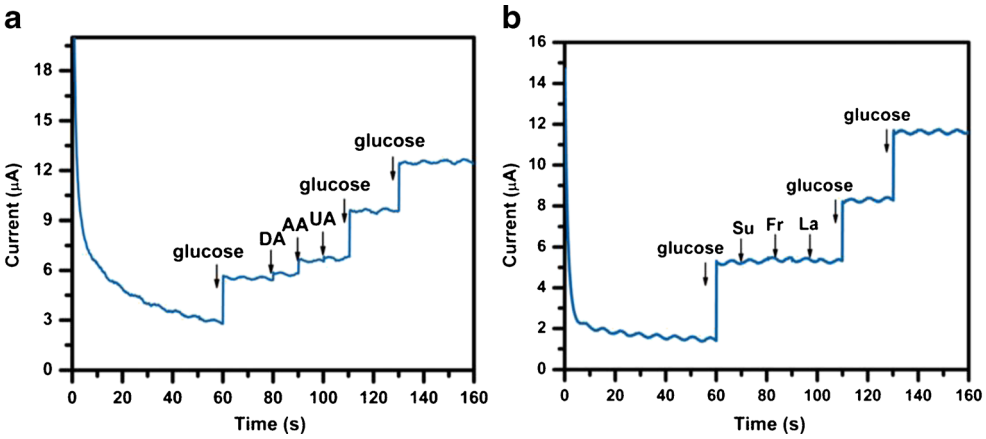

Fig. 5 Amperometric response of Pd-GWCNTs@GCE to successive addition of 1 mM glucose in presence of various interfering species such as (**a**) 0.1 mM dopamine, uric acid and ascorbic acid; (**b**) 0.1 mM lactose, fructose and sucrose at an applied potential of 0.05 V (vs. Ag/AgCl reference electrode)

concentration with $R^2 = 0.998$. The detection limit has been calculated to be 1 μM. The overall sensing activity of Pd-GWCNTs remarkably exceeds those reported Pd/graphene/CNT based glucose sensors [29–31]. This can be due to the combined synergistic effect of edge-plane like sites in GWCNTs and the uniformly anchored highly electrocatalytic Pd NPs. This intern results an enhanced electrocatalytic activity of the composite and furthermore ensures a fast charge transfer. Recent reports reveal that the interaction between adsorbed catalyst and carboneous substrate plays an important role in the activity enhancement of the catalyst [26].

Anti interference ability, stability and reproducibility of Pd-GWCNTs @GCE

The analytical performance of a sensor is graded by its ability to selectively detect the analyte by suppressing the signal from interference species. There are many easily oxidative electroactive species such as dopamine (DA), uric acid (UA), ascorbic acid (AA), lactose (La), fructose (Fr) and sucrose (Su), which normally coexist with glucose in human blood. As the normal physiological level of glucose is substantially higher (at least 10–30 times) than the interfering agents in human blood [32], we conducted the selectivity measurements of the as prepared Pd-GWCNTs@GCE sensor by repeatedly adding 1 mM glucose at 0.05 V, followed by successive addition of 0.1 mM of UA, AA, DA (Fig. 5a and 0.1 mM of Fr, La, Su (Fig. 5b) in 0.1 M NaOH solution under stirring conditions. It can be followed that the amperometric response for the interference species is very less compared to current obtained for glucose electrooxidation, which indicates that the fabricated Pd-GWCNTs@GCE sensor exhibits a good selectivity for glucose detection in the presence of interfering agents.

The stability of the amperometric current generated due to glucose electrooxidation is a potential factor in the analytical performance of the sensor. Any fluctuation deceives the glucose calibration. The stability of our Pd-GWCNTs@GCE sensor was investigated by measuring the signal durability for 5 mM glucose at 0.05 V over a long period of 4000 s (shown in Fig. S7 (A), ESI). As shown, no current fluctuation was observed, which depicts very good stability of the sensor. The inset (a) shows the plot representing the response time (time required to achieve ~99 % of steady state current) of the sensor, which is derived from i-t plot. It shows that the current stabilizes in no more than 0.1 s indicating excellent and rapid amperometric response behavior, which could be due to easy diffusion of glucose through modified electrode assembly and fast charge transfer at Pd-GWCNTs@GCE interface. Inset (b) depicts the amplified i-t plot in the specified area.

The reproducibility of the sensor was measured by monitoring the amperometric response of the same fabricated

Table 1 Comparison Table of applied potential, response time, detection limit and linearity range values for the present work showing significant improvements compared to various Pd/graphene/CNT based recent similar results

Materials	Methods used	Applied potential (V)	Response time (s)	Detection limit (μM)	Linearity range (mM)	Reference
Pd-GO	Ultrasonic	0.4	2	–	0.2–10	[23]
Pd-graphene	in situ reduction	0.4	9	1	0.01–5	[29]
Pd-FCNTs	Spontaneous reduction	0.4	–	–	0–46	[31]
Pd-SWCNTs	Chemical reduction	−0.35	3	0.2 ± 0.05	0.5–17	[33]
Pd-GWCNTs	Solar reduction	0.05	0.1	1	Up to 19.5	Present work

electrode for 1 mM glucose on each day over a period of 1 week, which is shown in Fig. S7 (B). It is worth mentioning that the electrode was rinsed thoroughly with DI water after each measurement and dried in ambient conditions. After 7 times repeated measurement, the final amperometric response remained approximately 84.5 % of its original value suggesting excellent reproducibility of the sensor.

The analytical performance of the fabricated sensor has been analyzed by comparing the calculated sensor parameters with the Pd based glucose sensors reported in literature (shown in Table 1). It can be observed that the linearity, working potential, response time are comparable or even better than similar sensing platforms. To be particular, the working potential and the response time are much lower than the other system. These excellent performances could be resulted from the synergistic effect from the surface anchored Pd NPs on highly protruded GWCNTs. On the one hand, GWCNTs provide enhanced electrochemical activity arising from the large number of edge-plane-like sites introduced by the wrinkles. On the other hand, the selective anchoring of PD NPs facilitate the glucose electroxidation, leading to a very low-potential glucose sensing platform.

Conclusion

Successful anchoring of Pd NPs on GWCNTs has been done by an one-step solar reduction technique. The fabricated sensor based on Pd-GWCNTs showed enhanced electrochemical properties, which facilitate enzyme-less glucose electroxidation at a very low working potential of +0.05 V, resulting from its enhanced electrocatalytic activity and rapid charge transfer. The sensor demonstrates excellent sensing performance for glucose with a wide linear calibration range, good reproducibility, a very fast response time and a low detection limit. In addition, it showed good selectivity, excellent reproducibility and outstanding stable amperometric response. Based on this outperformance, Pd-GWCNTs hybrid composite holds promise as a robust sensing matrix for a variety of potential applications that principally rely on enzyme-less glucose detection.

Acknowledgments The author thanks Indian institute of technology Madras (IITM), Chennai, India for financial support.

References

1. Steiner MS, Duerkop A, Wolfbeis OS (2011) Optical methods for sensing glucose. Chem Soc Rev 40:4805–4839. doi:10.1039/c1cs15063d
2. Wang J (2008) Electrochemical glucose biosensors. Chem Rev 108: 814–825. doi:10.1021/cr068123a
3. Turner APF (2013) Biosensors: sense and sensibility. Chem Soc Rev 42:3184–3196. doi:10.1039/c3cs35528d
4. Chen C, Xie Q, Yang D, Xiao H, Fu Y, Tan Y, Yao S (2013) Recent advances in electrochemical glucose biosensors: a review. RSC Adv 3:4473–4491. doi:10.1039/c2ra22351a
5. Pandya A, Sutariya PG, Menon SK (2013) A non enzymatic glucose biosensor based on an ultrasensitive calixarene functionalized boronic acid gold nanoprobe for sensing in human blood serum. Analyst 138:2483–2490. doi:10.1039/c3an36833e
6. Masoomi-Godarzi S, Khodadadi AA, Vesali-Naseh M, Mortazavi Y (2014) Highly stable and selective Non-enzymatic glucose biosensor using carbon nanotubes decorated by Fe_3O_4 nanoparticles. J Electrochem Soc 161:19–25. doi:10.1149/2.057401jes
7. Tan C, Huang X, Zhang H (2013) Synthesis and applications of graphene-based noble metal nanostructures. Mater Today 16:29–36. doi:10.1016/j.mattod.2013.01.021
8. Ye JS, Chen CW, Lee CL (2015) Pd nanocube as non-enzymatic glucose sensor. Sens Actuat B Chem 208:569–574. doi:10.1016/j.snb.2014.11.091
9. Mei H, Wu W, Yu B, Li Y, Wu H, Wang S, Xia Q (2015) Non-enzymatic sensing of glucose at neutral pH values using a glassy carbon electrode modified with carbon supported Co@Pt core-shell nanoparticles. Microchim Acta 182:1869–1875. doi:10.1007/s00604-015-1524-6
10. Hu FP, Wang Z, Li Y, Li C, Zhang X, Shen PK (2008) Improved performance of Pd electrocatalyst supported on ultrahigh surface area hollow carbon spheres for direct alcohol fuel cells. J Power Sources 177:61–66. doi:10.1016/j.jpowsour.2007.11.024
11. Sun T, Zhang Z, Xiao J, Chen C, Xiao F, Wang S, Liu Y (2013) Facile and green synthesis of palladium nanoparticles-graphene-carbon nanotube material with high catalytic activity. Sci Rep 3: 2527. doi:10.1038/srep02527
12. Yang W, Ratinac KR, Ringer SR, Thordarson P, Gooding JJ, Braet F (2010) Carbon nanomaterials in biosensors: should you use nanotubes or graphene? Angew Chem Int Ed 49:2114–2138. doi:10.1002/anie.200903463
13. Zhao L, Wu G, Cai Z, Zhao T, Yao Q, Chen X (2015) Ultrasensitive non-enzymatic glucose sensing at near-neutral pH values via anodic stripping voltammetry using a glassy carbon electrode modified with Pt_3Pd nanoparticles and reduced graphene oxide. Microchim Acta 182:2055–2060. doi:10.1007/s00604-015-1555-z
14. Lin Y, Lu F, Tu Y, Ren Z (2004) Glucose biosensors based on carbon nanotube nanoelectrode ensembles. Nano Lett 4:191–195. doi:10.1021/nl0347233
15. Neumann CCM, Batchelor-Mcauley C, Downing C, Compton RG (2011) Anthraquinone monosulfonate adsorbed on graphite shows two very different rates of electron transfer: surface heterogeneity Due to basal and edge plane sites. Chem Eur J 17:7320–7326. doi:10.1002/chem.201002621
16. Gong K, Chakrabarti S, Dai L (2008) Electrochemistry at carbon nanotube electrodes: is the nanotube Tip more active than the sidewall? Angew Chem Int Ed 47:5446–5450. doi:10.1002/anie.200801744
17. Dai X, Wildgoose GG, Compton RG (2006) Apparent 'electrocatalytic' activity of multiwalled carbon nanotubes in the detection of the anaesthetic halothane: occluded copper nanoparticles. Analyst 131:901–906. doi:10.1039/b606197d
18. Banks CE, Moore RR, Davies TJ, Compton RG (2004) Investigation of modified basal plane pyrolytic graphite electrodes: definitive evidence for the electrocatalytic properties of the ends of carbon nanotubes. Chem Comm 1804–1805. doi: 10.1039/B406174H
19. Tang L, Feng H, Cheng J, Li J (2010) Uniform and rich-wrinkled electrophoretic deposited graphene film: a robust electrochemical platform for TNT sensing. Chem Comm 46:5882–5884. doi:10.1039/c0cc01212b
20. Hummers WSJ, Offeman RE (1958) Preparation of graphitic oxide. J Am Chem Soc 80:1339. doi:10.1021/ja01539a017

21. Aravind SSJ, Eswaraiah V, Ramaprabhu S (2011) Facile synthesis of one dimensional graphene wrapped carbon nanotubes composites by chemical vapour deposition. J Mater Chem 21:15179. doi:10.1039/c1jm12731d
22. Baro M, Nayak P, Baby TT, Ramaprabhu S (2013) Green approach for the large-scale synthesis of metal/metal oxide nanoparticle decorated multiwalled carbon nanotubes. J Mater Chem A 1:482–486. doi:10.1039/c2ta00483f
23. Wang Q, Cui X, Chen J, Zheng X, Liu C, Xue T, Wang H, Jin Z, Qiao L, Zheng W (2012) Well-dispersed palladium nanoparticles on graphene oxide as a non-enzymatic glucose sensor. RSC Adv 2: 6245–6249. doi:10.1039/c2ra20425h
24. Nayak P, Anbarasan B, Ramaprabhu S (2013) Fabrication of organophosphorus biosensor using ZnO nanoparticle-decorated carbon nanotube-graphene hybrid composite prepared by a novel green technique. J Phys Chem C 117:13202–13209. doi:10.1021/jp312824b
25. Subrahmanyam KS, Manna AK, Pati SK, Rao CNR (2010) A study of graphene decorated with metal nanoparticles. Chem Phys Lett 497:70–75. doi:10.1016/j.cplett.2010.07.091
26. Sridhar V, Kim H, Jung J, Lee C, Park S, Oh I (2012) Defect-engineered three-dimensional graphene-nanotube-palladium nanostructures with ultrahigh capacitance. ACS Nano 6:10562–10570. doi:10.1021/nn3046133
27. Jia X, Hu G, Nitze F, Barzegar HR, Sharifi T, Tai C (2013) Synthesis of palladium/helical carbon nanofiber hybrid nanostructures and their application for hydrogen peroxide and glucose detection. ACS Appl Mater Interfaces 5:12017–12022. doi:10.1021/am4037383
28. Yuan W, Zhou Y, Li Y, Li C, Peng H, Zhang J, Liu Z, Dai L, Shi G (2013) The edge- and basal-plane-specific electrochemistry of a single-layer graphene sheet. Sci Rep 3:2248. doi:10.1038/srep02248
29. Lu LM, Li HB, Qu F, Zhang XB, Shen GL, Yu RQ (2011) In situ synthesis of palladium nanoparticle-graphene nanohybrids and their application in nonenzymatic glucose biosensors. Biosens Bioelectron 26:3500–3504. doi:10.1016/j.bios.2011.01.033
30. Qin Y, Kong Y, Xu Y, Chu F, Tao Y, Li S (2012) In situ synthesis of highly loaded and ultrafine Pd nanoparticles-decorated graphene oxide for glucose biosensor application. J Mater Chem 22:24821–24826. doi:10.1039/c2jm35321k
31. Chen XM, Lin ZJ, Chen DJ, Jia TT, Cai ZM, Wang XR, Chen X, Chen GN, Oyama M (2010) Nonenzymatic amperometric sensing of glucose by using palladium nanoparticles supported on functional carbon nanotubes. Biosens Bioelectron 25:1803–1808. doi:10.1016/j.bios.2009.12.035
32. Huang TK, Lin KW, Tung SP, Cheng TM, Chang IC, Hsieh YZ, Lee CY, Chiu HT (2009) Glucose sensing by electrochemically grown copper nanobelt electrode. J Electroanal Chem 636:123–127. doi:10.1016/j.jelechem.2009.08.011
33. Meng L, Jin J, Yang G, Lu T, Zhang H, Cai C (2009) Nonenzymatic electrochemical detection of glucose based on palladium-single-walled carbon nanotube hybrid nanostructures. Anal Chem 81: 7271–7280. doi:10.1021/ac901005p